ZenGen, a tool to generate ordered configurations for systematic first-principles calculations: The Cr–Mo–Ni–Re system as a case study

J.-C. Crivello, R. Souques, A. Breidi, N. Bourgeois, J.-M. Joubert

ZenGen☆: a tool to generate ordered configurations for systematic first-principles calculations, example of the Cr–Mo–Ni–Re system

J.-C. Crivello[a,*], R. Souques[a], N. Bourgeois[a], A. Breidi[a], J.-M. Joubert[a]

[a]*Chimie Métallurgique des Terres Rares (CMTR), Institut de Chimie et des Matériaux Paris-Est (ICMPE), CNRS UPEC UMR7182, 2–8 rue Henri Dunant, 94320 Thiais Cedex, France*

Abstract

"ZenGen" is a script-tool which helps to automatically generate first-principles input files of all the ordered compounds of a given crystal structure in a given system. The complete set of heats of formation of each end-member can then easily be used in the thermodynamic phase modeling. "ZenGen" is a free and open source code, which can be downloaded from http://zengen.cnrs.fr.

In order to illustrate its possibilities, the quaternary system, Cr–Mo–Ni–Re, has been investigated. The binary solid solution parameters have been estimated from SQS calculations. The $\sigma-$phase has been considered according to its crystal structure, *i.e.* with a 5-sublattice model, by the DFT calculation of the $4^5 = 1024$ different ordered quaternary configurations. Several tentative *ab initio* phase diagrams are presented.

Keywords: Calphad, DFT, CEF, intermetallic, sigma-phase

☆Fully documented manual and program are available on http://zengen.cnrs.fr.

*Corresponding author

Email address: crivello@icmpe.cnrs.fr (J.-C. Crivello)

1. Introduction

The field of thermodynamic modeling has been recently stimulated by the progress of techniques allowing the calculation of thermodynamic quantities from first-principles calculations, such as the Density Functional Theory (DFT) [1]. These methods allow the estimation of formation enthalpies of fully ordered compounds, taking into account their crystal structures. These calculations can be done not only for stable compounds, but also for metastable ones which play an important role in the description of these phases within the Compound Energy Formalism (CEF) [2, 3]. By using the CEF, any intermetallic phase could be described by a sublattice model for which every ordered configuration heat of formation has to be calculated. As an example, a binary phase with five crystal sites, described in a 5-sublattice model generates $2^5 = 32$ different ordered configurations, a ternary $3^5 = 243$ ... a huge number, but which can be calculated with today's super-computers.

Technically, performing calculations on a large number of end-members may cause two types of problems: (*i*) a mistake in the distribution of atoms among all different sites; (*ii*) a too fast relaxation of crystal structure, thus losing the initial symmetry. To avoid these kinds of errors, the "ZenGen" code was created. This code is able to generate all the necessary input files for the DFT calculations of the ordered configurations considering a given system. It has been tested on several phases, such as Laves phases ($C14$, $C15\ldots$), or other topologically close packed phases ($A12$, $A13$, $D8_b$, P, δ, $\ldots$). It can also be used to run Special Quasi-random Structures (SQS) calculations [4]. A basic introduction of Zengen workflow is given is section 2.

Then, in order to illustrate the ZenGen capacity, we have investigated the challenging quaternary Cr–Mo–Ni–Re system. Our aim was not to assess thermodynamically this system, but rather to show that systematic DFT calculations can be run contently in this very complex system, that they allow the calculation of a preliminary *ab initio* computed phase diagram, and that they can be used as an input for a traditional Calphad assessment . We have demonstrated this approach in our previous works [5, 6]. The results are presented in ~~the~~ section 3.

2. The ZenGen workflow

"ZenGen" is a free and open source code, governed by the CeCILL-B license under French law [7], which is officially recognized by Open Source Initiative (OSI). It can be downloaded from http://zengen.cnrs.fr. Zengen can be installed on Unix-Linux machines and uses Bash, Perl and Python languages. It has been designed to run VASP program [8, 9] for the DFT calculations, but could be adapted to other first-principles codes.

It requires as input the phase φ under consideration the crystallographic structure of which is constituted by m different sites, and the n different elements. Then, ZenGen decomposes the process into four steps:

1. Automatic generation of the input files for the n^m ordered configurations;
2. Setup of the convergence criteria and relaxation steps of the φ phase;
3. Job execution under the same conditions;
4. Collection of output results (total energy, crystallographic parameters) and generation of a TDB file.

These steps are shown schematically in the diagram of Figure 1 and are more detailed in the following paragraphs.

2.1. Generation of ordered configurations

After the command:

```
$ zengen.pl
```

the user should enter the name of the crystal structure (X= $C14$, *chi*−phase, SQS type...), and the name the chemical elements. The cut-off energy is also requested. For structures described by more than 2 nonequivalent sites, it is possible to merge sites in order to agree with a simplified sub-lattice description. Then, `zengen.pl` generates all the ordered configurations based on a simple algorithm which distributes atoms on all the inequivalent sites. The script separates the systems

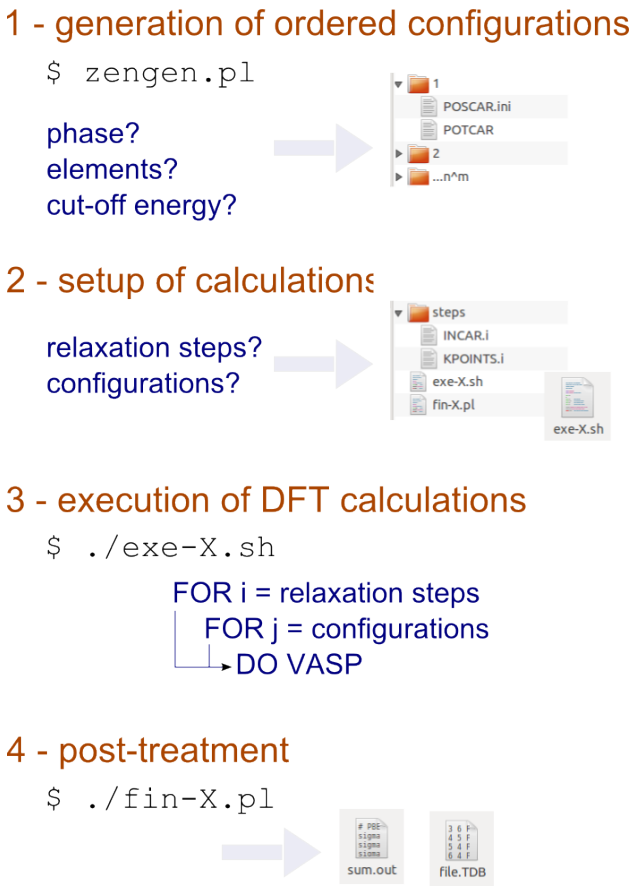

Figure 1: Schematic work flow chart of ZenGen.

(unary, binary, ternary...) and sorts the whole configurations by ascending the elemental composition. Finally, `zengen.pl` creates a folder containing all the ordered configurations labeled into subfolders (one by configuration), including all the files (`POSCAR` and `POTCAR`) needed to perform DFT calculations.

2.2. Setup of calculations

The calculation is built into 2 interlinked loops: one on the configurations to be calculated, one on the relaxation step. The `exe-X.sh` file has to be modified by the user regarding the particular demand: numeration of configuration and relaxation steps to be calculated . See the manual for more details.

2.3. *Execution of DFT calculations*

After the setup of the `exe-X.sh` file, its execution can be done in blind process mode by:

```
$ nohup ./exe-X.sh &
```

2.4. *Post-treatment*

After the calculations, the post-treatment is made by the command:

```
$ ./fin-X.pl
```

This script generates several files: a summary file `sum.out`, and a database file: `X.TDB`. The `sum.out` file contains the total energy, cell parameters, internal positions and magnetic moment of every configuration calculated by `exe-X.sh`. The `X.TDB` file can be used as an input file for thermodynamic calculation softwares, such as Thermo-Calc [10] or Open-Calphad [11]. It contains, for each configuration C in the φ phase, the corresponding formation energy, called $\Delta_f H^{\varphi}(C)$, given in Joule per formula unit, obtained by the difference between the total energies of $E^{\varphi}(C)$ and those of he weighted pure i elements in their standard element reference state (SER), E_i^{SER}:

$$\Delta_f H^{\varphi}(C) = E^{\varphi}(C) - \sum_i x_i \cdot E_i^{\mathrm{SER}} \tag{1}$$

The E_i^{SER} and $E_i^{\varphi}(\varphi = A1, A2, A3)$ have already been calculated with and without spin-polarization. They are provided for several cut-off energies (5 sets: 300, 400, 500, 600, and 800 eV) in the folder `pure` of the Zengen installation directory. Figure 2 shows the available i elements of the current version.

A user guide is available on the website http://zengen.cnrs.fr ("Documentation" page), including: the installation procedure, a tutorial, additional explanation, algorithm details, appendices...

Table 1 shows the available intermetallic phases in the current version. The list will probably be extended in future versions and the user may easily add its own structures.

ZenGen is designed to generate all necessary files for the calculation of ordered compounds described in the CEF formalism. However, it can also be used to prepare and execute SQS calculations of substitutional solid solutions. The SQS approach considers a random-like distribution of atoms on equivalent sites of a given lattice at a given composition and with a finite number of total atoms in the cell. This allows to express the mixing energy of the solid solution, $\Delta_{mix}H^{\varphi}$:

$$\Delta_{mix}H^{\varphi}(X) = E^{\varphi}(X) - \sum_{i=A,B} x_i \cdot E_i^{\varphi} \tag{2}$$

At the moment, only the *fcc*, *bcc*, and *hcp* ~~structures~~ phases for binary systems are implemented. Generated structures have been taken from the literature [12, 13, 14] respectively.

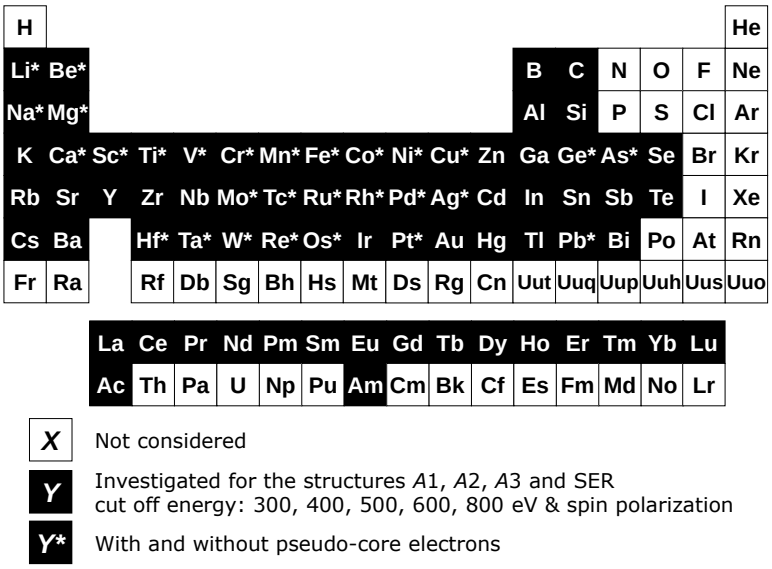

Figure 2: Periodic table showing the available elements in Zengen code (see `pure` folder).

Table 1: List of the available phases for calculation in ZenGen (code of the phase, Strukturbericht, prototype, Space group, Pearson symbol, number of sublattices and additional comments.

Code	Phase	Prototype	Space Group	Pearson	Nb	comments
chi	$A12$	$\alpha-$Mn	$I\bar{4}3m$ (217)	cI58	4	FK: $\chi-$phase
betaMn	$A13$	$\beta-$Mn	$P4_132$ (213)	cP20	2	$\beta-$Mn
A15	$A15$	Cr_3Si	$Pm\bar{3}n$ (223)	cP8	2	FK: $A15-Cr_3Si$
B2	$B2$	CsCl	$Pm\bar{3}m$ (221)	cP2	2	*bcc* ordered AB
B32	$B32$	NaTl	$Fd\bar{3}m$ (227)	cF16	2	*bcc* ordered AB
C14	$C14$	$MgZn_2$	$P6_3/mmc$ (194)	hP12	3	FK: Laves AB_2
C15	$C15$	Cu_2Mg	$Fd\bar{3}m$ (227)	cF24	2	FK: Laves AB_2
C36	$C36$	$MgNi_2$	$P6_3/mmc$ (194)	hP24	5	FK: Laves AB_2
D03	$D0_3$	BiF_3	$Fm\bar{3}m$ (225)	cF16	2	*bcc* ordered AB_3
sigma	$D8_b$	CrFe	$P4_2/mnm$ (136)	tP30	5	FK: $\sigma-$phase
mu	$D8_5$	Fe_7W_6	$R\bar{3}$ (166)	hR13	5	FK: $\mu-$phase
L10	$L1_0$	AuCu	$P4/mmm$ (123)	tP4	2	*fcc* ordered AB
L11	$L1_1$	CuPt	$R\bar{3}m$ (166)	hR6	2	*hex* ordered AB
L12	$L1_2$	$AuCu_3$	$Pm\bar{3}m$ (221)	cP4	2	*fcc* ordered AB_3
L21	$L2_1$	$AlCu_2Mn$	$Fm\bar{3}m$ (225)	cF16	3	*bcc* ordered ABC_2 Heusler
Cu3Ti		Cu_3Ti, Ni_3Ta	$Pmmn$ (59)	oP8	3	$\beta-Cu_3Ti$ (LT)
delta		Mo_7Ni_7	$P2_12_12_1$ (19)	oP56	12	FK: $\delta-$MoNi
Dsim		Mo_7Ni_7	$P2_12_12_1$ (19)	oP56	3	delta simplified [CN12,14,15+]
PP		$Cr_{18}Mo_{42}Ni_{40}$	$Pnma$ (62)	oP56	12	FK: P phase
PPsim		$Cr_{18}Mo_{42}Ni_{40}$	$Pnma$ (62)	oP56	3	P simplified [CN12,14,15+]
M		$Al_3Nb_{10}Ni_9$	$Pnma$ (62)	oP52	11	FK: M phase
R		$Cr_{16}Mo_{38}Co_{46}$	$Pnma$ (62)	hR159	11	FK: R phase

3. The Cr–Mo–Ni–Re system investigation

3.1. Known phase diagrams

The quaternary Cr–Mo–Ni–Re system is well suited for an automatic investigation of phase stability. Solid solutions with three different structures exists: $A1 - fcc$ (Ni), $A2 - bcc$ (Cr, Mo) and $A3 - hcp$ (Re), and two of elements are magnetic. The $\sigma-$phase is stable in the four ternaries. This phase is a hard brittle intermetallic compound and has a deleterious effect on the mechanical properties of many technologically important systems, like Cr-Mo-Ni-Re, a key system for Ni-based superalloys. The ternary iso-thermal sections have been drawn and compiled in the review of Slyusarenko [15]. Since this work, updates have been published and the most recent ternary phase diagrams are plotted in Figure 3.

3.2. DFT computational details

The $\sigma-$phase has been considered with a 5-sublattice model coresponding to its crystal structure and leading to the generation of $4^5 = 1024$ different ordered configurations. Initial crystallographic parameters have been taken from the reported average values [16]. Part of the work on the ternary systems has been published elsewhere ($\sigma-$CrMoRe [17], $\sigma-$CrNiRe [18], $\sigma-$MoNiRe [19]). However, to be sure that all calculations are done with the same parameters (cut-off energy...), they have been run for all the configurations. Solid solutions have been considered with the SQS approach to simulate the mixing of the binary solutions in fcc, bcc and hcp structures, for 0.25, 0.50 and 0.75 compositions with 16-atom supercells.

Thanks to ZenGen, the energy of every $\sigma-$phase end-member and SQS structure has been calculated by the DFT ~~calculation~~ approach using the Projector Augmented Wave (PAW) method [20], implemented in the Vienna Ab initio Simulation Package (VASP) [21, 22]. The exchange-correlation energy of electrons is described in the generalized gradient approximation (GGA) using the functional parametrization of Perdew-Burke-Ernzerhof [23]. The energy cut-off for the PAWs was set to 400 eV. All structures have been relaxed, keeping their original symmetries allowing only volume and cell shape evolution for σ and hcp symmetries. An additional step has been done allowing ionic relaxation. The final step included Blöchl corrections [24].

3.3. Thermodynamic modeling

3.3.1. Configuration energies of the $\sigma-$phase at 0 K

The $\sigma-$phase is described in the structure type FeCr, space group $P4_2/mnm$, 30 atoms per unit cell, with 5 inequivalent sites: $2a$, $4f$, $8i_1$, $8i_2$, $8j$, with coordination numbers (CN) 12, 15, 14, 12 and 14, respectively. The main feature of the $\sigma-$phase includes its non stoichiometry which is accommodated by substitution on different sites of the crystal structure [16], and its ability to accept wide homogeneity ranges. The main point of interest for the present work is that, qualitatively, in the $\sigma-$phase, larger atoms show preference for the sites with high coordination number (CN15 and CN14) whereas smaller atoms occupy the sites with low coordination number (CN12).

All the $4^5 = 1024$ configurations of the quaternary $\sigma-$phase have been considered by distributing the $n = 4$ atoms (Cr, Ni, Mo, Re) into the $m = 5$ sites (i, j, k, l, m). From the equation 1, the corresponding heat of formation, $\Delta_f H^{\sigma}_{ijklm}$, has been expressed relatively to the elements in their SER structure. All the results of the 1024 compositions, such as the relaxed crystallographic parameters and heats of formation, are given in a table as a supplementary material o this paper.

For each system (binary, ternary...), Table 2 gives selected configurations with smaller values of $\Delta_f H^{\sigma}_{ijklm}$. In comparison with previous works, slight differences are observed and are explained by the different exchange-correlation functions and cut-off energy. However, the same most stable configurations are found for each system. As an example, the only negative formation enthalpy in the binary systems is obtained in Mo–Ni system, for the Ni:Mo:Mo:Ni:Mo configuration (ideal Mo_2Ni composition) which corresponds to the occupation of low CN sites by Ni, (smaller atom) and high CN sites by Mo (larger atom).

This kind of geometric argumentation could be extended to the ternaries, such as in the Mo–Ni–Re system. From the $3^5 = 243$ configurations generated, 90 are unique compositions, and among them, 20 with $\Delta_f H^{\sigma}_{ijklm} < 0$, like the most stable configuration: Re:Mo:Re:Ni:Mo. They are all explained by the geometric argument. In fact, Ni whose atomic size is significantly smaller than Mo and Re prefers the sites with low coordination numbers *i.e.* $2a$ and $8i_2$ (CN12). On the other hand, Mo atoms being larger in size tend to occupy high coordination sites *i.e.* $4f$, $8i_1$ and $8j$ (CN15, 14, 14) where they find more space. Contrary to the behavior of Mo and Ni, the Re

atom, being intermediate in size r_{Ni} ($\sim$ 125 pm) < r_{Re} ($\sim$ 137 pm) < r_{Mo} ($\sim$ 139 pm), shows a dual preference depending on the composition.

Adding a fourth element makes analyses more complex. Cr size is intermediate between Ni and Re with a radius of about $\sim$ 128 pm. Only 8 quaternary configurations present a negative heat of formation. The most stable configurations are Cr:Re:Re:Ni:Mo, Cr:Mo:Mo:Ni:Re, or Cr:Mo:Re:Ni:Mo, explained by the discussion given earlier: larger atoms like Mo and Re prefer higher coordinated sites (CN14 and CN15), whereas smaller atoms like Ni and Cr prefer lower CN12 sites.

The valence electron number $\bar{e}$ has been given in Table 2. It has been discussed elsewhere [16, 25, 26] that $\bar{e}$ governs the stability of the $\sigma-$phase and has to be between 5.5 and 8 to make the phase stable. Since the less stable quaternay configuration (Re:Ni:Cr:Mo:Cr, $\Delta_f H > 30$ kJ/at) presents 6.6 valence electron and satisfies this electronic condition, it clearly shows that, even if the electronic argument may be important, the geometric one dominates strongly the $\sigma-$phase stability.

3.3.2. Ideal ternaries phase diagram

For the first calculation, ideal solid solutions have been considered. The Bragg-Wiliams-Gorsky approximation [29] has been applied using the CEF formalism to describe the $\sigma-$phase. Without any adjustable parameter and with DFT lattice stability of pure elements (only enthalpies no entropy terms), the four ternary phase diagrams have been calculated using the Thermo-Calc software package. They are represented in Figure 4. With the exception of Cr–Mo–Ni, all the expected $\sigma-$phases appear in a reasonable range of compositions.

3.3.3. Additional interaction parameters

Using the SQS results, the mixing enthalpy of binary solid solutions is obtained. As an example, the results on the three phases of Mo–Re are shown in Figure 5 The six binary systems will not be discussed in this work. From the mixing energy obtained after full relaxation, solutions have been treated as regular solutions with a fit done using a unique L^0 parameter. Results are summarized in Table 3, they have been considered for the computed ternary phase diagrams shown in Figure 6. The terminal solid solutions at each corner better match now the experimental

Table 2: Selected $\sigma-$phase configurations with average valence electron number $\bar{e}$ and their heat of formation $\Delta_f H^{\sigma}_{ijklm}$ (in kJ/at) calculated in the present study or in a previous works.

	System	$2a$ CN12	$4f$ CN15	$8i_1$ CN14	$8i_2$ CN12	$8j$ CN14	$\bar{e}$	$\Delta_f H^{\sigma}_{ijklm}$ calculated	$\Delta_f H^{\sigma}_{ijklm}$ previous works	Ref.
binaries	Cr-Mo	Cr	Mo	Mo	Cr	Mo	6.00	12.62	8.65	[17]
	Cr-Ni	Cr	Ni	Ni	Ni	Cr	8.67	7.63	5.65	[18]
	Cr-Re	Cr	Re	Re	Cr	Cr	6.40	0.60	1.00	[27]
		Cr	Re	Re	Cr	Re	6.67	0.79	1.30	[27]
	Mo-Ni	Ni	Mo	Mo	Ni	Mo	7.33	-0.67	-0.70	[19]
	Mo-Re	Re	Mo	Re	Re	Mo	6.60	0.96	1.07	[28]
	Ni-Re	Ni	Re	Re	Ni	Re	8.00	0.54	0.75	[18]
ternaries	Cr-Mo-Ni	Cr	Mo	Mo	Ni	Mo	7.07	0.65		
	Cr-Mo-Re	Cr	Mo	Re	Cr	Re	6.53	0.36	0.75	[17]
		Cr	Mo	Mo	Re	Re	6.53	-0.07	0.16	[17]
	Cr-Re-Ni	Cr	Re	Re	Ni	Cr	7.47	-2.11	-2.02	[18]
		Re	Re	Re	Ni	Cr	7.53	-1.28	-1.16	[18]
		Ni	Re	Re	Ni	Cr	7.73	-1.87	-1.80	[18]
	Mo-Ni-Re	Re	Mo	Re	Ni	Re	7.67	-0.85	-0.73	[19]
		Ni	Mo	Re	Ni	Re	7.87	-1.53	-1.42	[19]
		Ni	Re	Mo	Ni	Re	7.73	-0.14	-0.04	[19]
		Re	Re	Mo	Ni	Re	7.53	-0.73	-0.62	[19]
		Ni	Re	Re	Re	Mo	6.93	-0.50	-0.35	[19]
		Ni	Re	Re	Ni	Mo	7.73	-3.34	-3.25	[19]
		Re	Re	Re	Ni	Mo	7.53	-3.26	-3.15	[19]
		Mo	Re	Re	Ni	Mo	7.47	-1.44	-1.33	[19]
		Ni	Mo	Mo	Re	Re	6.80	-0.64	-0.50	[19]
		Ni	Mo	Mo	Ni	Re	7.60	-2.17	-2.09	[19]
		Re	Mo	Mo	Ni	Re	7.40	-2.93	-2.83	[19]
		Ni	Mo	Re	Ni	Mo	7.60	-3.52	-3.43	[19]
		Ni	Mo	Re	Re	Mo	6.80	-1.20	-1.06	[19]
		Re	Mo	Re	Ni	Mo	7.40	-3.50	-3.40	[19]
		Mo	Mo	Mo	Ni	Re	7.33	-1.10	-1.01	[19]
		Mo	Mo	Re	Ni	Mo	7.33	-0.53	-0.44	[19]
		Ni	Re	Mo	Ni	Mo	7.47	-0.60	-0.52	[19]
		Re	Re	Mo	Ni	Mo	7.27	-1.38	-1.29	[19]
		Re	Mo	Mo	Ni	Mo	7.13	-1.25	-1.18	[19]
		Ni	Mo	Mo	Re	Mo	6.53	-0.86	-0.74	[19]
quaternary	Cr-Mo-Ni-Re	Cr	Mo	Re	Ni	Re	7.60	-1.11		
		Ni	Mo	Re	Ni	Cr	7.60	-0.25		
		Re	Mo	Re	Ni	Cr	7.40	-0.24		
		Cr	Re	Mo	Ni	Re	7.47	-1.27		
		Cr	Re	Re	Ni	Mo	7.47	-3.07		
		Cr	Mo	Mo	Ni	Re	7.33	-2.37		
		Cr	Mo	Re	Ni	Mo	7.33	-2.01		
		Cr	Re	Mo	Ni	Mo	7.20	-0.49		
		Re	Ni	Cr	Mo	Cr	6.60	31.16		

measurements. However, the $\sigma-$phase does not appear in the Cr–Mo–Ni system, contrary to the experimental evidence [30]. Some adjusting parameters are needed to fix this point.

Using the same hypothesis, the quaternary phase diagram is plotted in Figure 7 in the form of several constant Ni-composition sections. This plot allows to evaluate the quaternary extension of the $\sigma-$phase. The most striking feature is the shrinking of the homogeneity range as a function of the Ni-content. In fact, Ni is the element richest in valence electrons (10 electrons). Thus, our result is in agreement with the empirical rule stating that the $\sigma-$phase forms for an average electron concentration range below the value of 8 [16, 26]

4. Conclusions

Zengen is a tool to automate the construction of the input files for the systematic DFT calculation of all the ordered configurations of a multicomponent phase. This approach can be used in parallel with a thermodynamic assessment of the system by the Calphad method. It has been illustrated by the calculation of the quaternary Cr–Mo–Ni–Re system for which all the binary solid solutions and every end-member of the quaternary $\sigma-$phase have been calculated for the first time.

Many improvements will be made in future versions of Zengen: creation of tools to easily add new structures, facilitate the site merging for sublattice description... At the present time, about fifty different users have downloaded the code, and Zengen has already been used by external people for different purposes, such as the study of the molar volume of the $\sigma-$phase involving transition elements [31], or the phase stability and mechanical properties of $\sigma-$phase in Co-Mo [32].

Acknowledgements

DFT calculations were performed using HPC resources from GENCI-CINES (Grant 2014-96175). Financial support, from the Agence Nationale de la Recherche (ANR), Project Armide ANR-10-BLAN-912-01 is acknowledged. N. Bourgeois is thankful to the French ANR agency for financial support from the national program Investments for Future ANR-11-LABX-022-01. The authors wish to thank Nathalie Dupin for useful and fruitful discussions.

Appendix A. Supplementary material

- DFT results of the $\sigma-$phase configurations (relaxed crystallographic parameters and heats of formation)
- Thermodynamic database file of Cr–Mo–Ni–Re (TDB format), including SQS results

References

[1] W. Kohn, Nobel lectures, chemistry 1996-2000, in: World Scientifc Publishing, Singapore, 2003.

[2] B. Sundman, B. J. Ågren, A regular solution model for phases with several components and sublattices, suitable for computer applications, J. Phys. Chem. Solids 42 (1981) 297–301.

[3] J.-O. Andersson, A. Guillermet, M. Hillert, B. Jansson, B. Sundman, A compound-energy model of ordering in a phase with sites of different coordination numbers, Acta Metall. 34 (3) (1986) 437–445.

[4] A. Zunger, S. H. Wei, L. G. Ferreira, J. E. Bernard, Special quasirandom structures, Phys. Rev. Lett. 65 (3) (1990) 353.

[5] J.-M. Joubert, J.-C. Crivello, M. Andasmas, P. Joubert, Phase stability in the ternary Re–W–Zr system, Acta Mater. 70 (0) (2014) 56–65.

[6] A. Breidi, M. Andasmas, J.-C. Crivello, N. Dupin, J.-M. Joubert, Experimental and computed phase diagrams of the Fe–Re system, J. Phys.: Condens. Matter 26 (48) (2014) 485402 (13p).

[7] CEA, CNRS, INRIA, CeCill-B license information, zengen IDDN.FR.001.280024.000.S.P.2015.000.10600, french Free Software license, compatible with the GNU GPL.
URL `http://www.cecill.info`

[8] G. Kresse, J. Hafner, Ab initio molecular dynamics for liquid metals, Phys. Rev. B 47 (1) (1993) 558–561.

[9] G. Kresse, J. Furthmüller, Efficient iterative schemes for ab initio total-energy calculations using a plane-wave basis set, Phys. Rev. B 54 (16) (1996) 11169–11186.

[10] B. Sundman, B. Jansson, J.-O. Andersson, The thermo-calc databank system, Calphad 9 (1985) 153–190.

[11] B. Sundman, U. Kattner, M. Palumbo, S. Fries, Opencalphad - a free thermodynamic software, Integrating Materials and Manufacturing Innovation 4 (1) (2015) 1.

[12] C. Wolverton, Crystal structure and stability of complex precipitate phases in Al-Cu-Mg(Si) and Al-Zn-Mg alloys, Acta Mater. 49 (16) (2001) 3129–3142.

[13] C. Jiang, C. Wolverton, J. Sofo, L.-Q. Chen, Z.-K. Liu, First-principles study of binary bcc alloys using special quasirandom structures, Phys. Rev. B 69 (2004) 214202.

[14] D. Shin, R. Arróyave, Z.-K. Liu, A. Van de Walle, Thermodynamic properties of binary hcp solution phases from special quasirandom structures, Phys. Rev. B 74 (2006) 024204.

[15] E. M. Slyusarenko, V. A. Borisov, M. V. Sofin, E. Y. Kerimov, A. E. Chastukhin, Determination of phase equilibria in the system Ni-V-Cr-Mo-Re at 1425 K using the graph method, J. Alloys Comp. 284 (1-2) (1999) 171–189.

[16] J.-M. Joubert, Crystal chemistry and calphad modeling of the σ phase, Prog. Mater. Sci. 53 (2008) 528–583.

[17] J.-C. Crivello, M. Palumbo, T. Abe, J.-M. Joubert, *Ab initio* ternary $\sigma-$phase diagram: the Cr-Mo-Re system, Calphad 34 (2010) 487–494.

[18] M. Palumbo, T. Abe, S. G. Fries, A. Pasturel, First-principles approach to phase stability for a ternary sigma phase: Application to Cr-Ni-Re, Phys. Rev. B 83 (14) (2011) 144109.

[19] K. Yaqoob, J.-C. Crivello, J.-M. Joubert, Study of site occupancies in Mo-Ni-Re sigma-phase by both experimental and ab initio methods, Inorg. Chem. 51 (2012) 3071–3078.

[20] P. E. Blöchl, Projector augmented-wave method, Phys. Rev. B 50 (24) (1994) 17953.

[21] G. Kresse, D. Joubert, From ultrasoft pseudopotentials to the projector augmented-wave method, Phys. Rev. B 59 (3) (1999) 1758.

[22] G. Kresse, J. Furthmüller, Efficiency of ab-initio total energy calculations for metals and semiconductors using a plane-wave basis set, Comput. Mater. Sci. 6 (1) (1996) 15–50.

[23] J. P. Perdew, K. Burke, M. Ernzerhof, Erratum: Generalized gradient approximation made simple, Phys. Rev. Lett. 78 (7) (1997) 1396.

[24] P. E. Blöchl, O. Jepsen, O. K. Andersen, Improved tetrahedron method for Brillouin-zone integrations, Phys. Rev. B 49 (23) (1994) 16223.

[25] B. Seiser, T. Hammerschmidt, A. N. Kolmogorov, R. Drautz, D. G. Pettifor, Theory of structural trends within 4d and 5d transition metal topologically close-packed phases, Physical Review B 83 (2011) 224116.

[26] B. Seiser, R. Drautz, D. Pettifor, TCP phase predictions in ni-based superalloys: Structure maps revisited, Acta Mater. 59 (2) (2011) 749–763.

[27] M. Palumbo, T. Abe, C. Kocer, H. Murakami, H. Onodera, Ab initio and thermodynamic study of the Cr-Re system, Calphad 34 (4) (2010) 495–503.

[28] J.-C. Crivello, J.-M. Joubert, First principles calculations of the σ and χ phases in the Mo-Re and W-Re systems, J. Phys.: Condens. Matter 22 (2010) 035402.

[29] W. L. Bragg, E. J. Williams, The effect of thermal agitation on atomic arrangement in alloys, Proceedings of the Royal Society of London. Series A 145 (855) (1934) 699–730.

[30] P. Turchi, L. Kaufman, Z.-K. Liu, Modeling of Ni-Cr-Mo based alloys: Part I- phase stability, Calphad 30 (1) (2006) 70 – 87.

[31] W. Liu, X.-G. Lu, Y.-L. He, L. Li, Modeling of molar volume of the sigma phase involving transition elements, Computational Materials Science 95 (0) (2014) 540–550.

[32] S. Li, J. Liu, B. Liu, Phase stability and mechanical properties of sigma phase in Co–Mo system by first princi-

ples calculations, Computational Materials Science 98 (0) (2015) 424–429.

[33] S. Saito, T. Takashima, K. Miyama, K. Kurokawa, T. Narita, Tie-lined compositions of the σ and (γ,δ) phases in the Re–Cr–Ni system at 1573 K, J. Japan Inst. Metals 75 (6) (2011) 361–365.

[34] K. Yaqoob, J.-M. Joubert, Experimental investigation of the Mo-Ni-Re system, J. Alloys Comp. 559 (2013) 101–111.

Table 3: Regular ${}^0L$ interaction parameter term (kJ/mol) obtained by SQS calculation. They are given for the six binary systems in the three structures : fcc, bcc, hcp.

	fcc	bcc	hcp
Cr–Mo	+9.8	+34.9	+42.3
Cr–Ni	-54.0	+26.3	-55.5
Cr–Re	-0.6	-17.2	+10.0
Mo–Ni	-54.2	+25.8	-54.0
Mo–Re	-18.1	-20.0	+2.9
Ni–Re	+7.2	-11.2	1.4

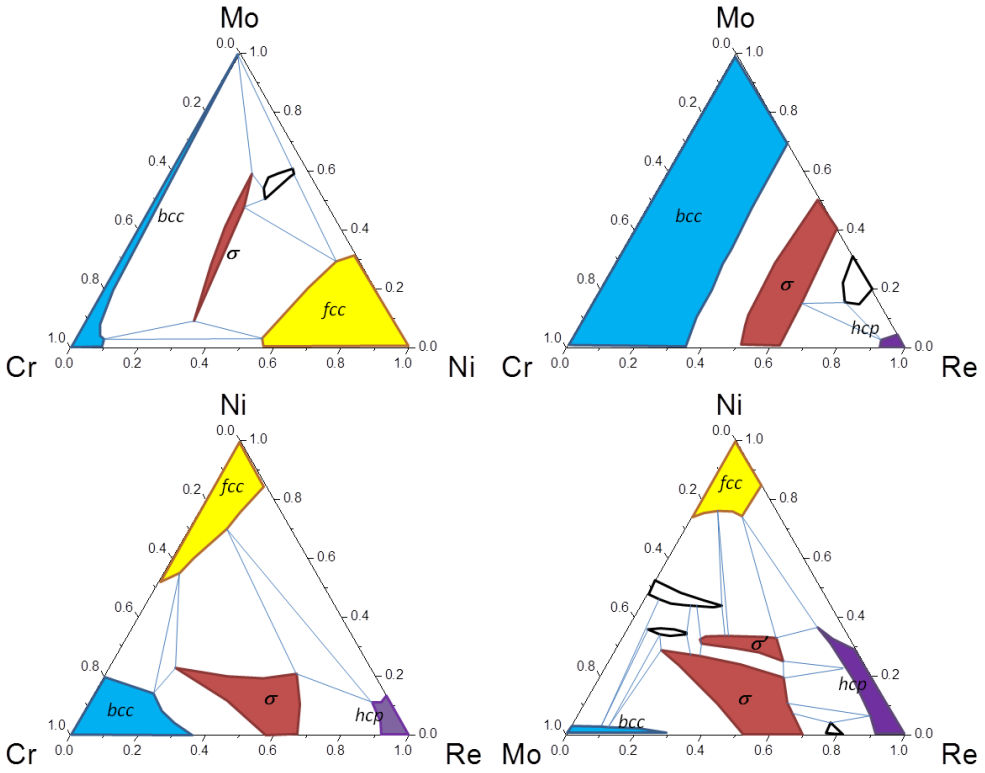

Figure 3: Literature ternary phase diagrams of Cr–Mo–Ni at 1323 K [30], Cr–Mo–Re at 1425 K [15], Cr–Ni–Re at 1573 K [33], Mo–Ni–Re at 1473 K [34]. Only solid solutions and the $\sigma-$phase are colored.

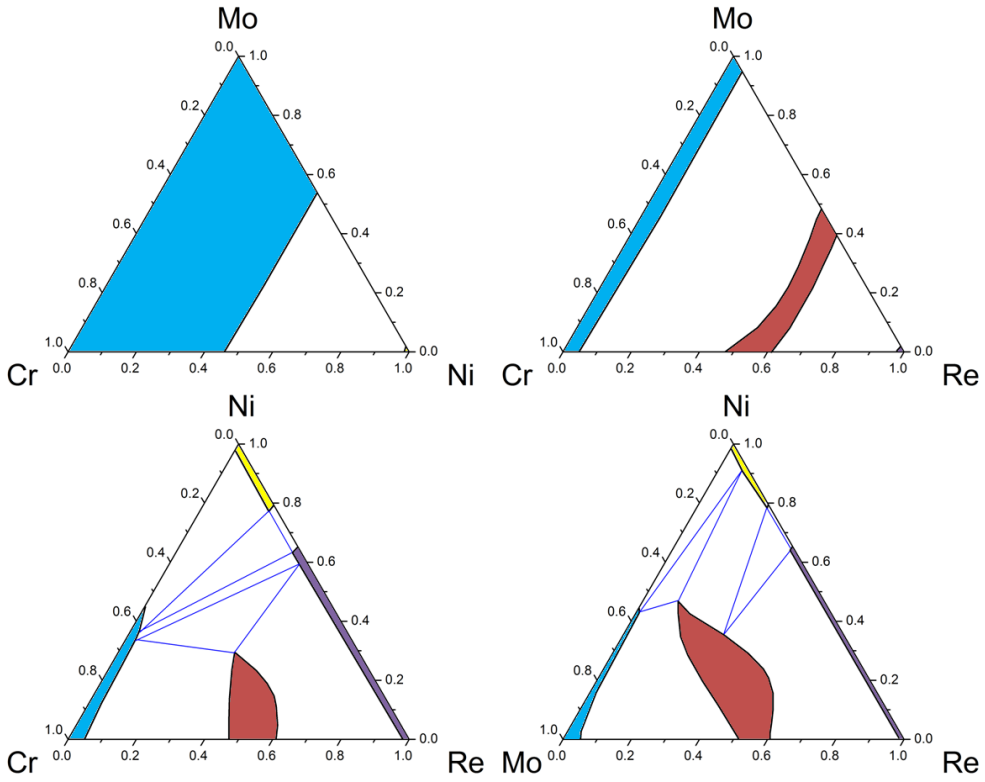

Figure 4: Using the BWG approximation, computed ternary phase diagrams of Cr–Mo–Ni, Cr–Mo–Re, Cr–Ni–Re and Mo–Ni–Re at 1423 K. The solid solutions are considered as ideal.

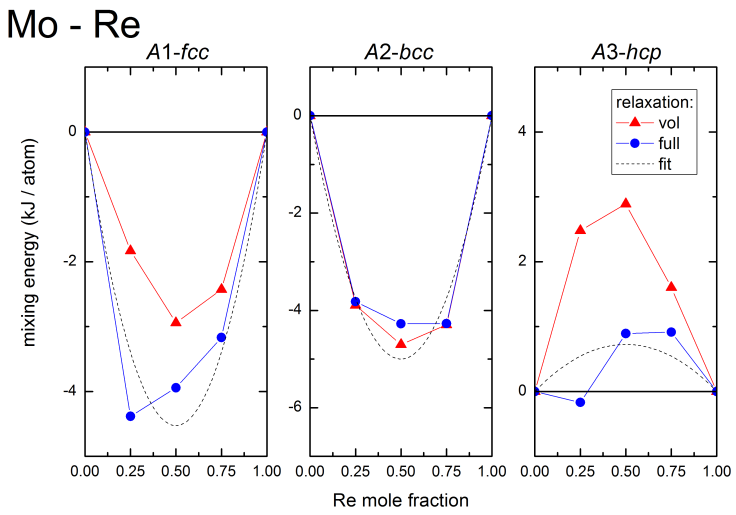

Figure 5: Enthalpy of mixing in the Mo–Re solid solutions calculated using SQS methodology of the three phases fcc, bcc and hcp. Dash line represents the fitted excess energy considered for the computed phase diagram.

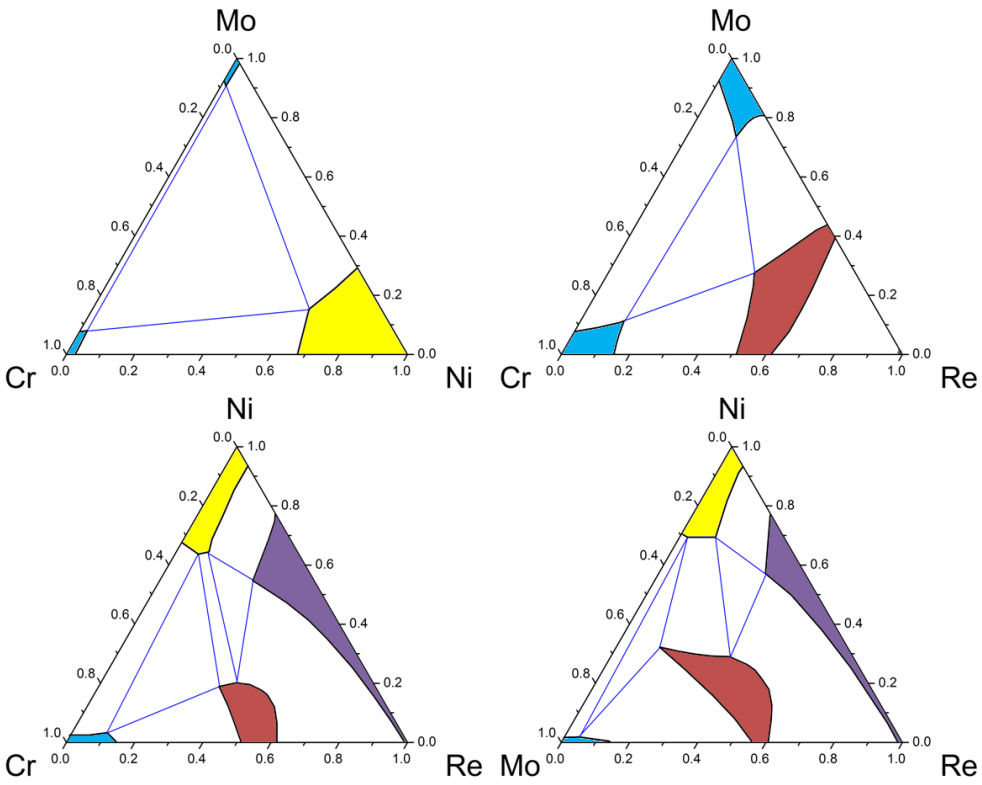

Figure 6: Computed ternary phase diagrams of Cr–Mo–Ni, Cr–Mo–Re, Cr–Ni–Re and Mo–Ni–Re at 1423 K. The solid solutions are considered as regular from the SQS results of Table 3.

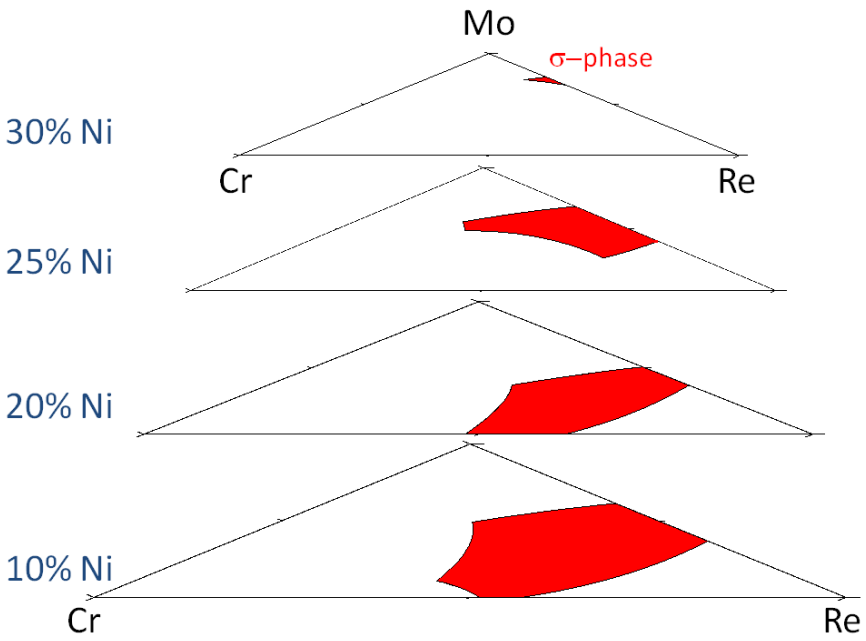

Figure 7: Computed quaternary Ni-isocomposition sections at 1423 K of Cr–Mo–Ni–Re phase diagrams for 10, 20, 25 and 30 at %-Ni.